RESUBMITTAL – DEVIATION FROM BWRVIP FLAW EVALUATION REQUIREMENTS FOR JET PUMP RISER INDICATION
Enclosure 2

NON-PROPRIETARY

Enclosure 2 is the redacted version of Enclosure 1

HITACHI

GE Hitachi Nuclear Energy

001N6043.5-NP
Revision 2
PLM Specification 001N6043 Revision 5
August 2015

Non-Proprietary Information – Class I (Public)

Energy Northwest
Columbia Generating Station
Jet Pump 17/18 Riser Evaluation at 106% Rated Core Flow (115 Mlbs/hr)

HITACHI

GE Hitachi Nuclear Energy

001N6043.5-NP
Revision 2
PLM Specification 001N6043 Revision 5
August 2015

Non-Proprietary Information – Class I (Public)

Energy Northwest
Columbia Generating Station
Jet Pump 17/18 Riser Evaluation at 106% Rated Core Flow (115 Mlbs/hr)

RESUBMITTAL – DEVIATION FROM BWRVIP FLAW EVALUATION REQUIREMENTS FOR JET PUMP RISER INDICATION
Enclosure 2

NON-PROPRIETARY

Enclosure 2 is the redacted version of Enclosure 1

INFORMATION NOTICE

This is a non-proprietary version of the document 001N6043.5, Revision 2, which has the proprietary information removed. Portions of the document that have been removed are indicated by an open and closed bracket as shown here [[ ]].

IMPORTANT NOTICE REGARDING CONTENTS OF THIS REPORT

Please Read Carefully

The design, engineering, and other information contained in this document are furnished for the purpose contained in the contract between Energy Northwest and GEH, and nothing contained in this document shall be construed as changing the contract. The use of this information by anyone other than Energy Northwest, or for any purpose other than that for which it is furnished by GEH is not authorized; and with respect to any unauthorized use, GEH makes no representation or warranty, and assumes no liability as to the completeness, accuracy, or usefulness of the information contained in this document.

REVISION SUMMARY

Rev.	Changes Incorporated in Current Version
0	Initial issue.
1	Revision created to address utility comments on Revision 0 of the report.
2	Revised EPRI proprietary marking.

Rev.	Previous Related Evaluations
0	GE Hitachi Nuclear Energy, "Justification for Continued Operation (JCO) for Columbia Generating Station with Jet Pump 17/18 Riser Pipe Flaw," NEDC-33689P, Revision 0, October 2011.
0	GE Hitachi Nuclear Energy, "Energy Northwest Columbia Generation Station Long Term Assessment of Columbia Generating Station Jet Pump 17/18 Riser Pipe Flaw at RS-9," 0000-0155-2198-R0, March 2013.

TABLE OF CONTENTS

ACRONYMS AND ABBREVIATIONS

Term	Definition
α	Flaw Half Angle
ΔK	Stress Intensity Factor
ΔK_{th}	Stress Intensity Threshold
σ_b	Applied FIV Axial Stress Range
σ_h	Hoop Stress
a	Half of the Axial Flaw Length
A-DELTA P	Accident Delta Pressure Force
ABS	Absolute Sum
AC	Acoustic Loads
AP	Annulus Pressurization (Loads)
ARTS	Average Power Range Monitor, Rod Block Monitor, Technical Specifications Improvement Program
ASME	American Society of Mechanical Engineers
BWR	Boiling Water Reactor
BWROG	BWR Owners' Group
BWRVIP	BWR Vessel and Internals Project
CGS	Columbia Generating Station
CHG	Chugging Loads
CLTP	Current Licensed Thermal Power
ECP	Corrosion Potential
DIR	Design Input Request
DRF	Design Record File
EPRI	Electric Power Research Institute
EVT-1	Enhanced VT-1
FIL	Flow Induced Loads
FIV	Flow Induced Vibration
GEH	GE Hitachi Nuclear Energy
gpm	Gallons per Minute
HAZ	Heat Affected Zone
HWC	Hydrogen Water Chemistry
IASCC	Irradiation-Assisted Stress Corrosion Cracking
ID	Inside Diameter
IGSCC	Intergranular Stress Corrosion Cracking
in.	Inch(es)

Term	Definition
in/hr	Inches per Hour
INR	Indication Notification Report
IVVI	In-Vessel Visual Inspection
JCO	Justification for Continued Operation
JP	Jet Pump
JR	Jet Reaction Loads
ksi	Kilo pounds per Square Inch
ksi $\sqrt{in}$	Kilo pounds per Square Inch – Square Root Inch
lb	Pound
LL	Limit Load
LOCA	Loss-of-Coolant Accident
MELLLA	Maximum Extended Load Line Limit Analysis
Mlbs/hr	Million Pounds per Hour
MPa-$m^{1/2}$	Mega Pascals - Square Root Meter
MOC	Method of Characteristics
mV_{she}	Unit of Coolant Conductivity (Milli-volt)
MWt	Megawatt Thermal
N-DELTA P	Normal Delta Pressure Force
N/A	Not Applicable
NDE	Non-Destructive Examination
NL	Metal + Water Weight + Hydraulic Loads (at 112.2% RCF) + Pressure Reaction Loads
NWC	Normal Water Chemistry
OBE	Operational Basis Earthquake
OD	Outside Diameter
OLTP	Original Licensed Thermal Power
OLNC	On-Line Noble Chemistry
P8B	Core Spray Weld Location per BWRVIP Nomenclature
P_{max}	Maximum Applied Stress
P_{min}	Minimum Applied Stress
PRC	Potentially Reportable Concern
psi	Pounds per Square Inch
PU	Power Uprate
R	Pipe Mean Radius
R	R-ratio
RCF	Rated Core Flow
RICSIL	Rapid Information Communication Services Information Letter

Term	Definition
RFO	Refueling Outage
RPV	Reactor Pressure Vessel
RS-9	Riser Weld Location per BWRVIP Nomenclature
SC	Safety Communication
SCC	Stress Corrosion Crack
SLO	Single Loop Operation
SRSS	Square Root of Sum of the Squares
SRV	Safety/Relief Valve Discharge Caused Loads
SSE	Safe Shutdown Earthquake
SX	Strain Gage X
t	Pipe Wall Thickness
TPO	Thermal Power Optimization
U-DELTA P	Upset Delta Pressure Force
UT	Ultrasonic Testing
VT-1	Visual Testing 1 (ASME Examination Standard)

1.0 Executive Summary

During the Columbia Generating Station (CGS) Spring 2011 refueling outage (RFO20) in-vessel visual inspection (IVVI) a crack indication of 1.25 inches in length at an angle of 62.6 degrees off the horizontal on Jet Pump 17/18 (JP-17/18) riser pipe in the proximity of the RS-9 weld was reported (References 1, 2, and 3). This flaw was evaluated in 2011 and was re-evaluated in 2013 at various operating conditions. The 2013 evaluation determined that the flaw was acceptable with limitations on the total core flow. In 2014, a re-evaluation of the flaw at 106% rated core flow (RCF) (115 Mlbs/hr) was requested (Reference 1).

Because operation at 106% RCF could not be supported using the standard intergranular stress corrosion cracking (IGSCC) crack growth rate of 5×10^{-5} in/hr as required by BWR Vessel and Internals Project (BWRVIP) letter 2012-074 (Reference 4), a reduced IGSCC crack growth rate was justified (see Section 5.1). The reduced IGSCC crack growth rate of [[ ]] was justified for [[

]] Therefore the expected growth after one cycle of the crack tip [[

]]. The total expected length of the flaw after one cycle is [[ ]]. Because the indication is oriented at an angle of 63 degrees, the flaw length is decomposed into its circumferential and axial components, as shown in Table 1-1.

For the 106% RCF flow induced vibration (FIV) loads the fatigue allowable flaw lengths were calculated and are also shown in Table 1-1. Previous analyses (References 5 and 6) included a limit load (LL) analysis at 112.2% RCF (which bounds the 106% RCF conditions) to calculate an allowable LL flaw size to assure no plastic collapse or failure under the normal operating and design accident loads. The LL allowable flaw lengths in the circumferential and axial directions are given in Table 1-1.

Table 1-1 Summary of Calculated Allowable Flaw Lengths and Comparison with the Projected Flaw Component Lengths

Flaw Length	Circumferential Flaw	Axial Flaw
Existing Flaw Projected after 1 Cycle	[[ ]]	[[ ]]
FIV Fatigue Allowable Length (106% RCF)	[[ ]]	[[ ]]
Projected Component Length < FIV Allowable Length	Yes	Yes
LL Allowable Length (112.2% RCF)	[[ ]]	[[ ]]
Projected Component Length < LL Allowable Length	Yes	Yes

The projected circumferential length of the flaw after one cycle of operation is [[ ]]. The projected axial length of the flaw after one cycle of operation is [[ ]]. Table 1-1 shows that for operation at 106% RCF, the FIV allowable circumferential length is [[ ]] and the FIV allowable axial length is [[ ]]. Both component allowable lengths are greater than the respective projected component length of the flaw after one cycle. The LL evaluation considered a conservative and bounding RCF of 112.2% RCF. For operation at 112.2% RCF, the LL allowable circumferential length is [[ ]] and the LL allowable axial length is [[ ]]. Both component allowable lengths are greater than the respective projected component length of the flaw after one cycle.

The CGS JP-17/18 riser crack indication leakage was also evaluated (References 7 and 8) considering 112% RCF, which bounds 106% RCF. The results of the leakage assessment indicated that JP-17/18 crack leakage has a negligible effect on core flow and a minor effect on JP flow.

Therefore, the as-found indication (1.25 inches measured length) is acceptable for one cycle (two years in duration) of operation considering 106% RCF. To account for long-term operation, re-inspection is required at every outage and if the indication's measured length of 1.25 inches does not increase, this evaluation can be used for the next cycle.

2.0 Scope

During the CGS Spring 2011 refueling outage (RFO20) IVVI (Reference 1) a crack indication of 1.25 inches in length at an angle of 62.6 degrees off the horizontal (Reference 3) on JP-17/18 riser pipe in the proximity of the RS-9 weld (Reference 2) was reported. This flaw was evaluated in 2011 and was re-evaluated in 2013 (see Section 3) for various operating conditions. In 2014, a re-evaluation of the flaw at 106% RCF (115 Mlbs/hr) was requested (Reference 1).

Because operation at 106% RCF could not be supported using the standard IGSCC crack growth rate of 5 x 10^{-5} in/hr per BWRVIP letter 2012-074 (Reference 4), a reduced IGSCC crack growth rate needs to be justified.

[[

]]

3.0 Introduction and Background

During the CGS Spring 2011 refueling outage (RFO20) IVVI (Reference 1), a crack indication of 1.25 inches at an angle of 62.6 degrees off the horizontal (Reference 3) on JP-17/18 riser pipe in the proximity of the RS-9 weld (Reference 5) was reported. This flaw was evaluated in 2011 and was re-evaluated in 2013 for a long-term assessment. A summary of these previous evaluations is provided below.

3.1 Background on JP-17/18 Configuration and RS-9 Indication

The JP assembly (Reference 9) is a part of the reactor recirculation system. As shown in Figure 3-1, each assembly consists of a riser assembly, a riser brace, two inlet-mixer assemblies, and two diffuser assemblies. Each assembly is installed in the annulus between the reactor pressure vessel (RPV) and the shroud. There are 20 JPs (10 JP assemblies) installed at CGS.

The indication is on JP-17/18 riser pipe in the proximity of the RS-9 weld left corner radius (JP-17 side) and transitions upward around the riser pipe towards JP-18, as shown in Figures 3-2 and 3-3. According to the guidelines of American Society of Mechanical Engineers (ASME) Code Section XI, Appendix C (Reference 10), the skewed riser flaw is projected onto a circumferential plane (a plane perpendicular to the riser pipe axis) and an axial plane (a plane containing the riser pipe axis). The axial and circumferential components of the flaw obtained by these projections were evaluated separately.

Based on past experience, two potential cracking mechanisms were considered: (1) IGSCC, and (2) high-cycle fatigue from FIV loading. IGSCC in boiling water reactor (BWR) components is typically located in weld HAZs, and tends to propagate random branches. The observed indication initiated in the HAZ and progressed away from the weld HAZ. Based on a review of earlier inspection tapes, the cracking was present as early as RFO15, conducted in 2001. Considering the observation that the flaw apparently did not increase in length since 2001 (RFO15) over the 10 years to the current inspection in 2011 (RFO20) and showed no growth between RFO20 and RFO21 (References 11 and 12), the inclusion of future IGSCC crack growth is conservative.

The original design basis requires three-point contact at the inlet mixers. Two restrainer bracket wedges (also known as auxiliary wedges) were installed in JP-18 in 1997 and two auxiliary wedges were installed in JP-17 in 2011 (References 11 and 13). Therefore, three-point contact is assumed in this evaluation. To mitigate slip joint leakage flow instability, two slip joint clamps were installed on JP-17 and JP-18 in 2005 (Reference 13). The FIV loads on this modified configuration were calculated at the JP-17/18 riser pipe near the RS-9 weld by using the plant start-up test data of the original design basis configuration (Reference 14).

Per BWRVIP-28-A (Reference 15), large recirculation line breaks loss-of-coolant (LOCA) are the only breaks that are potentially affected by the cracked JP riser pipes. The core shroud and JPs form a boundary that allows the core to reflood to a level of approximately two-thirds core height (approximately the top of the JP inlet mixer nozzles). The JP riser is the main component providing structural integrity to JP assemblies.

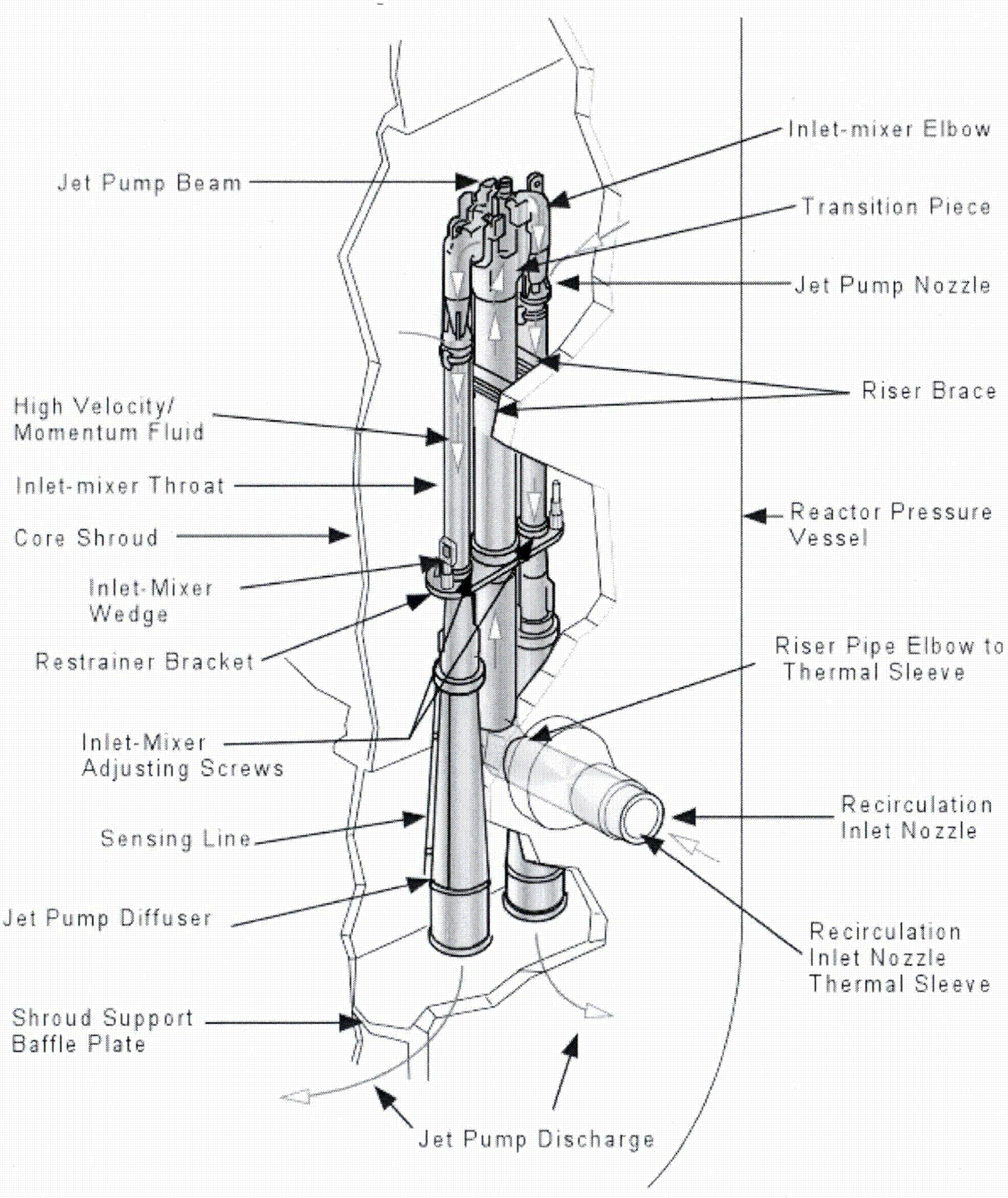

Figure 3-1 Typical JP Assembly (Reference 9)

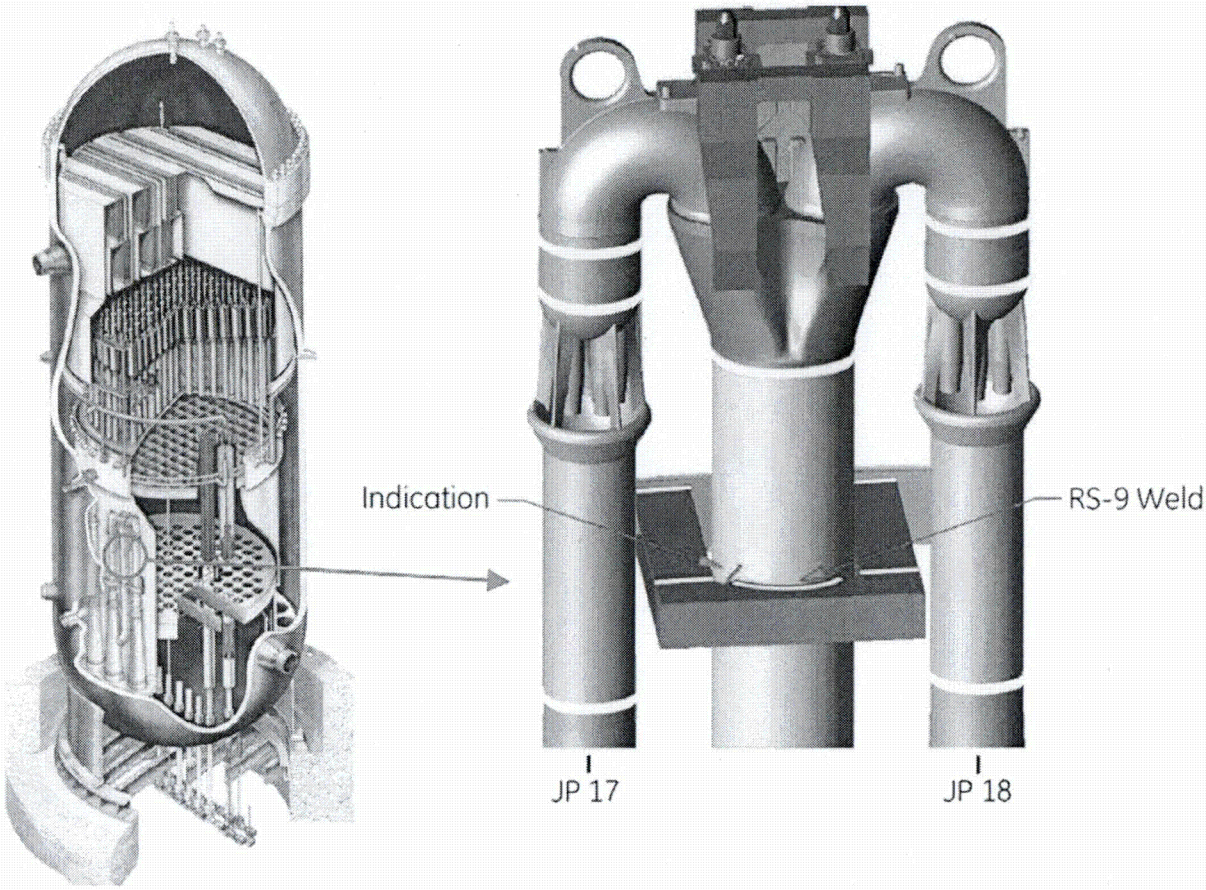

Figure 3-2 Schematic of JP-17/18 Riser Pipe Crack Indication (Reference 2)

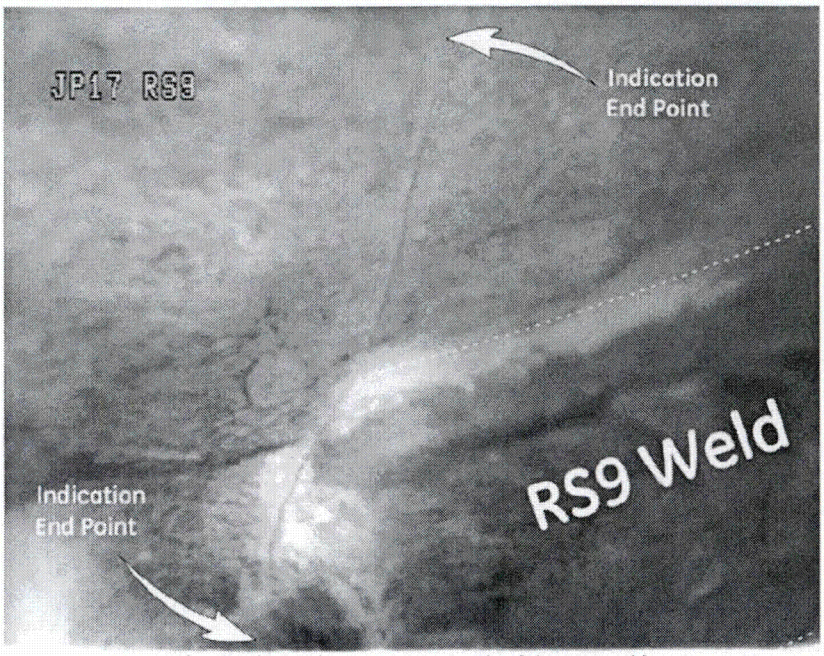

Indication located on Jet Pump 17 side of the RS-9 weld

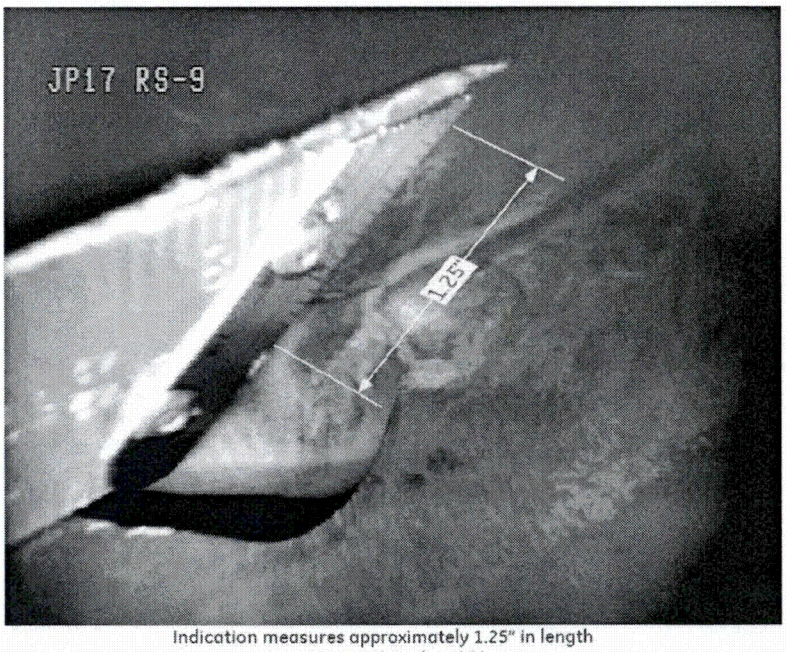

Indication measures approximately 1.25" in length
Measurement Scale in 1/16" Divisions

Figure 3-3 Inspection Results of JP-17/18 Riser Pipe Crack Indication (Reference 2)

3.2 Background of 2011 Evaluation

A flaw evaluation was performed (Reference 5) to provide a justification for continued operation (JCO) for one fuel cycle (two years in duration) of operation with the presence of the 1.25-inch long flaw on JP-17/18 RS-9.

3.2.1 2011 Evaluation Key Assumptions and Inputs

The key assumptions and inputs for this evaluation are provided in Table 3-1.

Table 3-1 2011 Evaluation Key Assumptions and Inputs

1	103% RCF (111.8 Mlbs/hr) operating conditions for FIV load analysis
2	112.2% RCF for LL and leakage analyses
3	Measured indication is 1.25 inches in length, 62.6 degrees off of horizontal
4	[[ ]]
5	IGSCC crack growth rate = [[ ]] (as justified by the utility in the design input request (DIR) (Reference 16))
6	IGSCC crack growth rate = [[ ]] (as justified by the utility in the DIR (Reference 16))
7	Measurement uncertainty = [[ ]]
8	Cycle length = 2 years
9	JP maintains original design configuration three point contact (set screw gap is 0 inch and/or wedges installed)
10	Safety Communication (SC) 09-01 considered in loads evaluation

3.2.2 2011 Evaluation Analysis and Results

During the JCO evaluation (Reference 5) the total flaw length was assumed to be 1.69 inches which includes the measured length of 1.25 inches (at 62.6 degrees off of the horizontal) (Reference 3) plus [[ ]] of IGSCC crack growth [[ ]] during one cycle at a rate of [[ ]], based on effective hydrogen water chemistry (HWC), in the same direction as the flaw (Reference 16). [[ ]] Per BWRVIP letter 2009-135 as authorized in Reference 16, non-destructive examination (NDE) measurement uncertainty [[ ]] in the evaluation. Because the indication was assumed to be oriented at an angle of 62.6 degrees, the flaw length was decomposed into its circumferential and axial components, as shown in Table 3-2.

In the 2011 evaluation, the FIV loads were calculated for the upper bound power uprate (PU) and 103% of the RCF (111.8 Mlbs/hr) with equal loop flows of 55.9 Mlbs/hr in each loop. A LL analysis was also performed at 112.2% RCF to calculate an allowable flaw size to assure no plastic collapse or failure under the normal operating and design accident loads. Table 3-2 summarizes the calculated allowable flaw lengths for each condition as compared to the projected one fuel cycle (two years in duration) circumferential and axial flaw lengths.

Table 3-2 Summary of 2011 Calculated Allowable Flaw Lengths and Comparison with the 2011 Projected Flaw Lengths (Reference 5)

Flaw Length	Circumferential Flaw (inches)	Axial Flaw (inches)
Existing Flaw Projected after 1 Cycle	[[	
FIV Fatigue Growth Allowable (103% RCF)		
LL Allowable (112.2% RCF)		
Allowable Flaw/Projected Flaw (FIV) (103% RCF)		
Allowable Flaw/Projected Flaw (LL) (112.2% RCF)		]]

For the 2011 evaluation, the projected circumferential length of the flaw after one cycle of operation was [[ ]]. The projected axial length of the flaw after one cycle of operation was [[ ]]. Table 3-2 shows that for operation at 103% RCF, the FIV allowable circumferential length was calculated to be [[ ]] and the FIV allowable axial length was [[ ]]. Both component allowable lengths were greater than the respective projected component length of the flaw after one cycle, as represented by the ratio of the allowable flaw length to the projected flaw length being greater than one. The LL evaluation considered a conservative and bounding RCF of 112.2% RCF. For operation at 112.2% RCF, the LL allowable circumferential length was [[ ]] and the LL allowable axial length was [[ ]]. Both component allowable lengths were greater than the respective projected component length of the flaw after one cycle.

The CGS JP-17/18 riser crack indication leakage was also evaluated. The results of the leakage assessment indicated that JP-17/18 crack leakage has a negligible effect on core flow and a minor effect on JP flow (Reference 5).

3.3 Background of 2013 Evaluation

In 2013, a fracture mechanics evaluation was performed to support long-term operation (Reference 6).

For the long-term evaluation, a different approach was used because the goal was to determine the maximum long term allowable flaw length using the standard IGSCC crack growth rate (Reference 5).

3.3.1 2013 Evaluation Key Assumptions and Inputs

The key assumptions and inputs for this evaluation are provided in Table 3-3.

Table 3-3 2013 Evaluation Key Assumptions and Inputs

1	98% RCF (106.3 Mlbs/hr) and 103% RCF (111.8 Mlbs/hr) operating conditions for FIV load analysis
2	112.2% RCF for LL and leakage analyses
3	Measured indication is 1.25 inches in length, 62.6 degrees off of horizontal
4	[[ ]]
5	IGSCC crack growth rate = 5 x 10^{-5} in/hr [[ ]]
6	IGSCC crack growth rate = 5 x 10^{-5} in/hr [[ ]]
7	Measurement uncertainty = [[ ]]
8	Cycle length = 2 years
9	JP maintains original design configuration three point contact (set screw gap is 0 inch and/or wedges installed)
10	Incorporates GEH SC 12-20 and SC 09-01 considered in loads evaluation

3.3.2 2013 Evaluation Analysis and Results

During the long-term assessment (Reference 17), the total flaw length was assumed to be 3.00 inches which included the measured length of 1.25 inches (at 62.6 degrees off of the horizontal) (Reference 6) plus [[ ]] of IGSCC crack growth ([[ ]]) incurred during one cycle of operation. The [[ ]] of growth was the result of standard IGSCC crack growth rate of 5 x 10^{-5} in/hr per BWRVIP letter 2012-074 (Reference 18) applied to both crack tips per BWRVIP-41 (References 19, 20, and 6). Per BWRVIP letter 2009-135 as authorized in Reference 16, NDE measurement uncertainty [[ ]] in the evaluation. Because the indication was assumed to be oriented at an angle of 62.6 degrees, the flaw length was decomposed into its circumferential and axial components, as shown in Table 3-4.

In the 2013 evaluation, the FIV loads were calculated for 98% of the RCF (106.33 Mlbs/hr) with equal loop flows of 53.17 Mlbs/hr in each loop and for the upper bound RCF of 103% (111.8 Mlbs/hr) with 55.9 Mlbs/hr in each loop. A LL analysis was also performed at

112.2% RCF to calculate an allowable flaw size to assure no plastic collapse or failure under the normal operating and design accident loads. Table 3-4 summarizes the calculated allowable flaw lengths for each condition as compared to the projected one fuel cycle (two years in duration) circumferential and axial flaw lengths.

Table 3-4 Summary of 2013 Calculated Allowable Flaw Lengths and Comparison with the 2013 Projected Flaw Lengths (Reference 6)

Flaw Length	Circumferential Flaw	Axial Flaw
Existing Flaw Projected after 1 Cycle	[[	
FIV Fatigue Length Allowable (98% RCF)		
Allowable Flaw/Projected Flaw (FIV) (98% RCF)		
FIV Fatigue Length Allowable (103% RCF)		
Allowable Flaw/Projected Flaw (FIV) (103% RCF)		
LL Length Allowable (112.2% RCF)		
Allowable Flaw/Projected Flaw (LL) (112.2% RCF)		]]

For the 2013 evaluation, the projected circumferential length of the flaw after one cycle of operation was [[ ]]. The projected axial length of the flaw after one cycle of operation was [[ ]]. Table 3-4 shows that for operation at 98% RCF, the FIV allowable circumferential length was calculated to be [[ ]] and the FIV allowable axial length was [[ ]]. For operation at 103% RCF, the FIV allowable circumferential length was calculated to be [[ ]] and the FIV allowable axial length was [[ ]]. Both component allowable lengths were greater than the respective projected component length of the flaw after one cycle, as represented by the ratio of the allowable flaw length to the projected flaw length being greater than one. The LL evaluation considered a conservative and bounding RCF of 112.2% RCF. For operation at 112.2% RCF, the LL allowable circumferential length was [[ ]] and the LL allowable axial length was [[ ]]. Both component allowable lengths were greater than the respective projected component length of the flaw after one cycle, as represented by the ratio of the allowable flaw length to the projected flaw length being greater than one.

The CGS JP-17/18 riser crack indication leakage was also evaluated. The results of the leakage assessment indicated that JP-17/18 crack leakage has a negligible effect on core flow and a minor effect on JP flow (Reference 17).

4. FIV Evaluation

In this section, the riser pipe loads (forces and moments) at the crack location under various operating conditions are evaluated. These are inputs to the fracture mechanics evaluation in the next section. It is assumed with slip joint clamps and auxiliary wedges installed, that the JP-17/18 assembly has been returned to its original as-designed condition (i.e., three point contact). [[

]] The operating conditions considered for the loads are taken from the power/core flow map shown in Figure 4-1 (Reference 21).

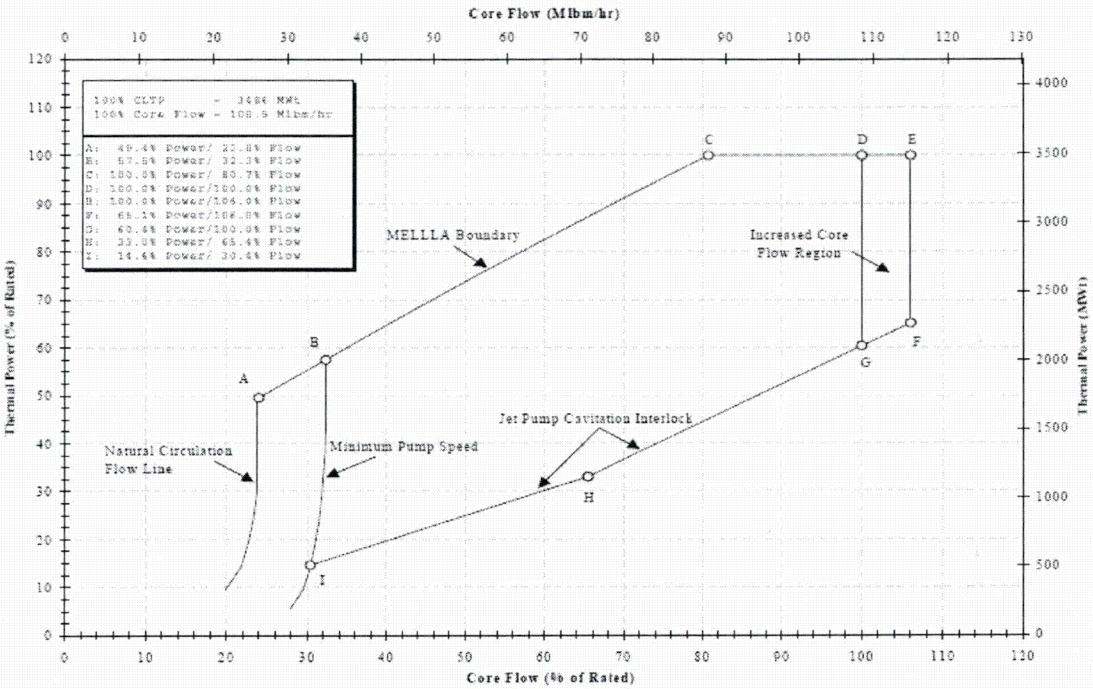

Figure 4-1 Power Flow Map Operating Conditions Evaluated (Reference 21)

The FIV loads were calculated at the JP-17/18 riser pipe near the RS-9 weld by using the plant start-up test data of the original design basis configuration. [[

]] The 100% core flow (108.5 Mlbs/hr) loads and moments data in Reference 14 were further adjusted [[

]]. Note that the FIV loads were not loads reduced by average power range monitor, rod block monitor, Technical Specifications improvement program (ARTS) / maximum extended load line limit analysis (MELLLA). [[

]] Thus the increase in FIV loads at 106% RCF from CLTP to TPO is insignificant, leading to an insignificant change in the FIV allowable flaw lengths. Also, note that the inclusion of ARTS/MELLLA may provide additional margin because the ARTS/MELLLA loads are not the most conservative loads (Reference 22).

4.1 Plant Vibration Measurements and Extrapolation

CGS is a BWR/5 reactor with a 251-inch diameter vessel. The FIV startup data in the CGS (Hanford-2) reactor internals vibration measurements report (Reference 23) is used in the calculations for the riser brace load components. At CGS, [[ ]] were used to record vibrational strains at the riser braces, and signals were processed in prescribed combinations to obtain the complete state of strain in radial and tangential modes (Reference 14). The frequency data from NEDE-30995P (Reference 23) is applicable for this evaluation because the vibration frequencies are not affected by operational changes since the startup data was gathered.

In the data analysis, the measured vibration amplitudes at dominant frequencies were compared to the allowable limits derived from the natural vibration modes of the component. For each vibration frequency, the location of the highest stress was identified and the allowable vibration limits for all the gage locations were established from the corresponding analytical mode shapes. The vibration limits were determined by setting the maximum zero to peak stress amplitude of the mode to 10 ksi, including the effects of stress concentration. The 10 ksi stress limit used for the Type 304 steels of the BWR internals is lower than the most conservative value allowed by the current ASME Section III design codes for the same material, which is 13.6 ksi for service cycles in excess of 10^{11} cycles (Reference 14).

The riser brace stresses at each JP mode under the operating conditions are generated by an extrapolation method using the CGS start up test data (Reference 23) for riser brace sensor [[ ]] under test conditions with [[ ]] core flow. [[ ]] data are used because they present the highest stresses among all instrumented JPs (Reference 14).

The riser brace stress values for [[ ]] core flow are first adjusted to the proper flow rate of the considered operating condition by [[ ]]. The riser brace stresses of the [[ ]] JP modes are considered as these are the dominant modes of vibration. There are two methods to combine the modal results. [[

]]

4.2 JP Model and Derivation of Riser Pipe Loads

The riser pipe forces and moments at the weld RS-9 location are obtained from Reference 14. Based on the dimensions of the JP assembly (References 24 and 25), a structural dynamic finite

element model was developed and analyzed using the engineering computer program SAP4G07 (Reference 26). This is a GEH Level 2 program. The model was benchmarked against the measured startup test data (Reference 23) as explained in Reference 27. [[ ]] The maximum strains during startup were recorded in the riser braces. The maximum riser brace stress at different core flows and [[ ]] original licensed thermal power (OLTP) was computed. A random time history (white noise) of duration [[ ]] and digitized at [[ ]] was used to represent temporal distribution of annulus pressures around JPs. The JP model was analyzed for the above random time history with the force scale factors developed from JP [[ ]]. The transient response analysis using modal superposing time history analysis was performed. The analysis used a time step of [[ ]] and a total of [[ ]] time steps. The modal damping ratio is [[ ]] (Reference 28). The analysis results for the riser stresses were benchmarked with the in-plant start-up test measurements. The time history loads are scaled up or down to match with the measured riser brace stress.

The riser pipe loads (forces and moments) above the yoke at [[ ]] RCF are given in Table 4-1. All loads tabulated are (0-peak) amplitude values. These loads are input to the fracture mechanics evaluation in Section 5. Note that single loop operation (SLO) is not specifically considered for this evaluation (i.e., SLO is not an equipment-out-of-service option evaluated). However if SLO occurs, the recommendations in Rapid Information Communication Services Information Letter (RICSIL) 092 (Reference 29) should be followed. Specifically, the loop flow in Operating Loop B should be brought back to a value less than or equal to one half maximum allowed core flow for two loop operation (½ of 115 Mlbs/hr or 57.5 Mlbs/hr) within [[ ]] hours. If the plant is required to manually trip a recirculation pump, such as to mitigate unplanned equipment performance degradation or similar concerns, the core flow should be reduced prior to the manual trip so that the remaining active JP loop flow will be less than or equal to one half of the maximum allowed core flow for two loop operation (½ of 115 Mlbs/hr or 57.5 Mlbs/hr) (Reference 14).

Table 4-1 FIV Riser Pipe Loads Above the Brace Yoke at 106% RCF

	Axial	Shear Radial RPV	Shear Tangent RPV	Torque	Moment Bending About RPV Radial	Moment Bending About RPV Tangential
Load from the riser pipe above brace yoke – with equal loop flows at [[ ]] RCF	[[					]]

5.0 Fracture Mechanics Evaluation

Fracture mechanics analysis is performed to determine the acceptability of the riser pipe flaw including the potential of flaw growth due to FIV cyclic fatigue and stress corrosion crack (SCC) under sustained load, or a combination of both for one fuel cycle of operation.

Based on the analysis guidelines of ASME Code Section XI, Appendix C (Reference 10), flaws that do not lie in either an axial or a circumferential plane should be projected onto these planes. The axial and circumferential flaws obtained by these projections should be evaluated separately. The evaluation required the geometries of the components of JP-17/18 defined in References 24 and 25 and a projection of the end of cycle crack length considering IGSCC.

5.1 Crack Growth Rate Determination

The Spring 2011 refueling outage (RFO20) IVVI notification report (Reference 1) described the flaw as a crack indication 1.25 inches long at an angle of 62.6 degrees off the horizontal (Reference 3) on JP-17/18 riser pipe in the proximity of the RS-9 weld (Reference 2). In the subsequent Spring 2013 inspection, the indication was re-examined and found to have not changed, remaining at 1.25 inches total length (Reference 16). For flaw evaluations, the standard crack growth rate (used historically for core shrouds and other reactor internals) is a rate of 5×10^{-5} inches/hr. However, for the CGS RS-9 weld indication, a more realistic IGSCC crack growth rate can be justified based on several factors. While the specific environmental conditions at the RS-9 location vary from other locations of reactor internal components, the factors that form the basis for this re-assessment of the IGSCC growth rate are as follows: [[

]] The following discussion will review these factors which support a reduced rate in place of the standard growth rate of 5×10^{-5} inches/hr. This reduced rate will then be used in the fracture mechanics evaluation in the next section of the report.

5.1.1 Material and Environment

The riser pipe, attached to the riser brace yoke is [[ ]] stainless steel. Therefore the welding process between the pipe and yoke created a HAZ where sensitization occurred. The HAZ region is expected to be limited to approximately [[ ]] inch from the weld fusion line, based on previous assessments in other BWR components. Given its location in the annulus region, the pipe is irradiated during operation which influences the material microstructure. However, the fluence levels at the JP location are lower than those associated with the fluence levels at the core shroud and have a smaller effect on material properties in the HAZ. As stated in BWRVIP-41, irradiation-assisted stress corrosion cracking (IASCC) is not a concern during the original licensing period. It is expected that the fluence level will only reach the IASCC limit of 5×10^{20} n/cm^2 in the later years of operation during

license renewal as stated in BWRVIP-234. However, the CGS end of license (54 EFPY) fluence in the JP riser pipe region is estimated to be 2.53 x 10^{20} n/cm^2 (Reference 18). This is less than the IASCC threshold (5 x 10^{20} n/cm^2). Therefore IASCC is not a concern for this evaluation during the current license period (54 EFPY).

In relation to the water chemistry environment, CGS is an on-line noble chemistry (OLNC) plant, and so it is considered to be mitigated with optimum hydrogen additions.

5.1.2 Previous Inspection Results at CGS

The major factors prompting the re-evaluation of the crack growth rates are the results of the last two visual inspections as well as a re-assessment of the inspection results of the crack location performed several outages earlier. Table 5-1 lists the results of both of the documented inspections in 2011 and 2013 (Reference 30). The last two detailed enhanced VT-1 (EVT-1) inspections were documented and used to show there were no changes in crack length between inspections. Additionally, based on a review of earlier inspection tapes, the cracking was present as early as RFO15 conducted in 2001 even though no length could be determined (RS-9 comparison document from Reference 18). The last two detailed EVT-1 inspections were documented and used to show there were no changes in crack length between inspections. Both indication notification reports (INRs) characterized the total length to be 1.25 inches as stated earlier. In support of these assessments, Figures 5-1a, 5-1b and 5-2 show the images taken from the inspection tapes and INRs respectively. The last two clearly substantiate the statement that no growth has occurred, thereby establishing the primary basis for revising the crack lengthening rate that can be used in the fracture mechanics evaluation discussed in the next section of the report.

The findings at CGS are consistent with other findings in BWRs. Specifically, re-inspections of an RS-9 indication present in a BWR/4 in 2002 and 2010 following the discovery of cracking in 2000, established no measureable growth even though the plant operated with no additional restrictions. This is very similar to the results of the inspections at CGS.

Table 5-1 CGS JP-17/18 RS-9 Inspection Data

Inspection/ Outage	INR Number	Crack Length (inches)	Crack Length Change (inches)	Calculated Growth Rate (inches/hr)	Comments
RFO15	N/A	No specific length assigned	N/A	N/A	Digital enhancement shows indication
RFO20	CGS-R20-IVVI-11-07	1.25	N/A	N/A	Clear documentation
RFO21	CGS R21-IVVI-13-01, R2	1.25	0	0	Re-inspection confirms no changes

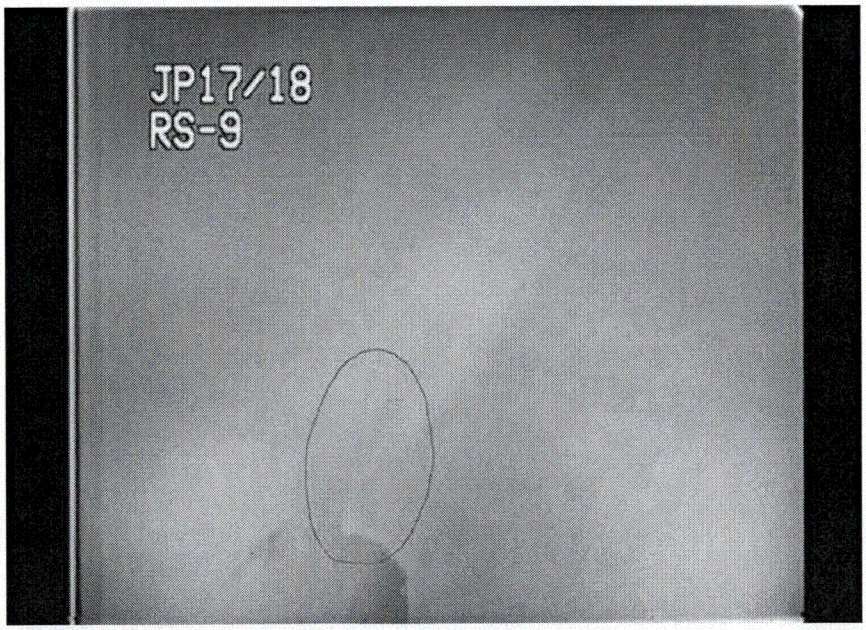

Figure 5-1a RFO15 Image Digitally Enhanced to Highlight the RS-9 Indication

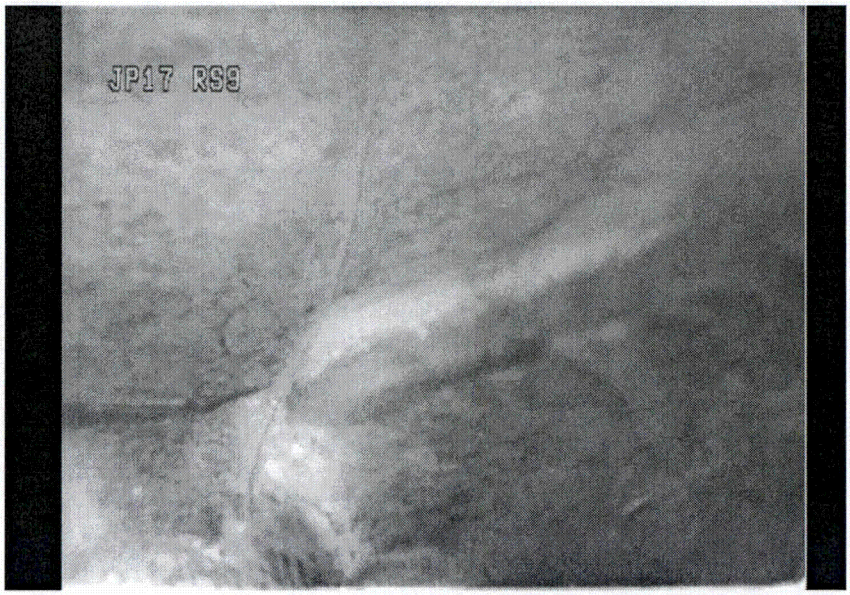

Figure 5-1b RFO20 Image of the Indication on JP-17/18 Riser RS-9 Weld

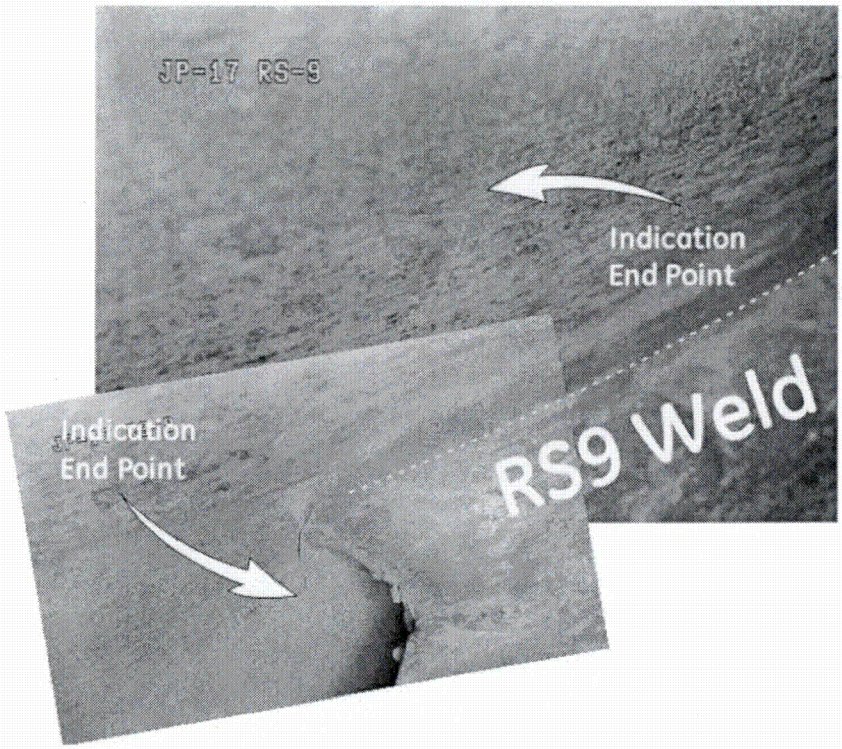

Figure 5-2 RFO21 Image of the Indication on JP-17/18 Riser RS-9 Weld

5.1.3 Core Spray Piping IGSCC Crack Growth Rates from BWRVIP-224

The core spray piping, while somewhat smaller diameter than the riser piping in all types of BWRs, was also constructed using Type 304 material with the exception of the BWR/6 plants. Efforts were made to evaluate crack growth rates based on ultrasonic testing (UT) re-inspection data by the BWRVIP in conjunction with GEH (Reference 31). This data provides crack growth rates that are very applicable given that they were measured in piping versus shrouds. While the core spray location does not experience any significant irradiation, it is a location above the top guide that is not mitigated by the effective OLNC/HWC present adjacent to the RS-9 flaw. The crack growth rates in the core spray piping exposed to a normal water chemistry (NWC) environment are greater than those for the JP assembly exposed to irradiation under HWC conditions, based on BWRVIP-14 model predictions (Reference 32).

Figure 5-3 displays the cumulative crack growth rates measured in those non-creviced core spray welds that exhibited cracking and required re-inspection (Reference 31). Recognizing that [[ ]] of the welds did not show any further growth, the figure shows that [[ ]] of the entire distribution were bounded by a rate of [[ ]] with [[ ]] of the data bounded by [[ ]]. Figure 5-4 shows the same data along with the crack growth rates for the entire population, which includes the rate measurements associated with the core spray P8b creviced welds (Reference 31). The data establish that for this expanded basis, [[ ]] of the rates for the cumulative distribution were [[ ]] or less.

[[

]]

Figure 5-3 Crack Growth Rates Determined in Core Spray Piping Welds Excluding the Creviced P8b Welds

Note: [[ ]] of the rates are [[ ]]. This is the data presented in Figure 5-4 of BWRVIP-224 (Reference 31)

[[

]]

Figure 5-4 BWRVIP-224 (Reference 31) Figure 5-4 Showing All Crack Growth Rates Determined in Core Spray Piping Welds Including the Creviced P8b Welds

Note: For [[ ]] of all welds, the crack growth rates are [[ ]].

5.1.4 Core Shroud OD IGSCC/IASCC Growth Rates per BWRVIP-174, Revision 1

The next comparison is shown in Figure 5-5, displaying the data presented in BWRVIP-174, Revision 1 (Reference 33). These data, also presented in a cumulative fashion and based on UT re-inspection data, are for the mitigated shroud outside diameter (OD) lengthening rates. The cumulative data is based on UT re-inspection data used to calculate crack growth rates for the mitigated OD for the horizontal shroud welds. These data points are very representative of the JP location with respect to fluence and environment. The data is bounded at [[ ]] with a growth rate of [[ ]] similar to the core spray data. While the core shroud is a different configuration, it is relevant in supporting a reduced crack growth rate for the JP weld location because the shroud welding process also introduces both sensitization and tensile residual stresses similar to the JP riser welds. The data also shows that [[ ]] of the indications, once detected, did not exhibit subsequent growth in the re-inspection when mitigated.

[[

]]

Figure 5-5 Data from Figure 5-4 of BWRVIP-174, Revision 1 (Reference 33) Showing the Core Shroud OD Crack Lengthening Growth Rates with Effective Mitigation

Notes: For [[ ]] of all welds, the lengthening rates are [[ ]]. This is similar to the core spray lengthening rates.

In the three IGSCC flaw length studies/cases, shown in Figures 5-3 through 5-5 and described above, the [[ ]] values are significantly less than the conservative 5×10^{-5} in/hr IGSCC value typically used as the standard crack growth rate in the length direction. The GEH review determined that [[ ]] of the [[ ]] for the IGSCC crack growth rate data; therefore, it can be used to justify a reduced crack growth rate of [[ ]].

5.1.5 Expected IGSCC Crack Growth Rates in Non-Sensitized Type 304 Stainless Steel in HWC Environment

As initially stated the existing IGSCC crack tip currently lies outside of the conventional HAZ and, as such, is growing into non-sensitized material. This condition has been shown in laboratory tests to significantly reduce the crack growth rate as well. Figure 5-6, taken from Reference 32, shows crack growth rate data for stainless steel as a function of material condition and corrosion potential. The triangles, derived from annealed material, are well below the rates

measured in the sensitized material, represented by the colored triangles. This difference is at least a factor of [[ ]]. The data in this figure also shows the effect of the lower corrosion potential. For a range of coolant conductivities in the fully mitigated environment, defined to be [[ ]], the crack growth rate is well over an order of magnitude slower as determined at a stress intensity factor of [[ ]], a value that could be present on the pipe OD surface for an existing crack. In summary, both the lack of sensitization and the low corrosion potential (ECP) will lead to lower rates of crack lengthening as the crack grows following its existing trajectory. These factors provide significant support for the use of a lower crack lengthening rate as well.

[[

]]

Figure 5-6 From NEDC-32985P, Figure 5.1-25 (Reference 32)

5.1.6 Proposed IGSCC Crack Growth Rate for Use in CGS JP-17/18 RS-9 Assessment

As stated earlier, several factors need to be considered in defining a lower crack growth rate that can be used in the prediction of the crack length in the CGS JP-17/18 riser pipe during the next operating cycle. A reduced IGSCC crack growth rate is supported by the lack of any crack growth in the last several outages, consistent with the majority of crack indications in core spray piping weld HAZs and core shroud OD weld HAZs. Additionally, given that the crack indication tip lies in non-sensitized material and is exposed to a mitigated environment, the crack indication is expected to arrest or grow slowly.

Based on the data from the few indications that did lengthen based on re-inspections, both in the core spray piping welds and the shroud OD weld HAZs, a crack growth rate of [[ ]] is considered appropriate for the 106% RCF assessment of the CGS RS-9 weld indication at both tips.

For conservatism in this evaluation, the reduced IGSCC crack growth rate of [[ ]] is used outside of the HAZ region (upper crack tip) and the standard BWRVIP-accepted crack growth rate of 5×10^{-5} in/hr per Reference 4 is used within the HAZ region (lower crack tip).

5.2 2014 Evaluation Inputs and Assumptions

The key assumptions and inputs for this evaluation are provided in Table 5-2.

Table 5-2 2014 Evaluation Key Assumptions and Inputs

1	106% RCF (115 Mlbs/hr) operating conditions for FIV load analysis
2	112.2% RCF for LL and leakage analyses
3	Measured indication is 1.25 inches in length, 63 degrees off of horizontal
4	[[ ]]
5	IGSCC crack growth rate = 5 x 10^{-5} in/hr [[ ]]
6	IGSCC crack growth rate = [[ ]]
7	Measurement uncertainty = [[ ]]
8	Cycle length = 2 years
9	JP maintains original design configuration three point contact (set screw gap is 0 inch and/or wedges installed)
10	Incorporates GEH SC 09-01, 11-07 (considered but not applicable, see Section 5.5.1), 12-20, and 14-02
11	[[ ]]

5.3 Projected End of Cycle Flaw Length

In this evaluation for 106% RCF, crack growth due to IGSCC is considered at both ends of the flaw. The projected total flaw length is calculated to be [[ ]] which includes the measured length of 1.25 inches (at 63 degrees off of the horizontal) (Reference 3) [[ ]] 5 x 10^{-5} in/hr [[ ]] Per BWRVIP letter 2009-135 as authorized in Reference 16, NDE measurement uncertainty is [[ ]] in the evaluation. Because the indication is oriented at an angle of 63 degrees, the flaw length is decomposed into its circumferential and axial components, as shown in Table 5-4. These are the flaw lengths that were used to compare to the FIV fatigue growth and LL threshold flaw lengths.

5.4 FIV Allowable Flaw Length Evaluation

Consistent with the methodology used in References 5 and 6, to predict the potential of any FIV cyclic fatigue crack growth, a threshold stress intensity factor, ΔK_{th}, is defined for the circumferential and axial components of the flaw length. The FIV fatigue allowable flaw length is calculated such that the resulting stress intensity factor is equal to the threshold stress intensity factor, ΔK_{th}. For a given flaw size and FIV load, if the calculated stress intensity factor, ΔK, is less than the ΔK_{th}, then fatigue crack growth due to high cycle loading such as FIV is not predicted.

The ΔK_{th} of a material is a function of the R-ratio. The R-ratio, an indication of the relative magnitudes of the mean and the fluctuating stresses, is defined as

$$R = P_{min}/P_{max},$$

where P_{min} and P_{max} are the applied minimum and maximum stresses, respectively. The R-ratios were calculated using the maximum hydraulic-induced stress (Reference 34), steady state pressure, and the calculated alternating hoop stress. For the circumferential component of the flaw, the R-ratio is calculated to be 0.15, and the generally accepted corresponding ΔK_{th} for Type 304 stainless steel material is 5 ksi $\sqrt{in}$ (References 35 and 36). For the axial component of the flaw, the R-ratio is calculated to be 0.88, and the corresponding ΔK_{th} for Type 304 stainless steel material is 3 ksi $\sqrt{in}$ (Reference 35).

5.4.1 FIV Allowable Circumferential Flaw

For the FIV fatigue growth "threshold crack length" calculation, a through-wall circumferential flaw is assumed. The stress intensity factor, ΔK, for a given FIV axial stress range (peak-to-peak) is calculated from the relation (References 36 and 37):

$$\Delta K = \sigma_b (\pi R\alpha)^{0.5} F_b$$

where

$$F_b = 1 + A[4.596 (\alpha/\pi)^{1.5} + 2.6422 (\alpha/\pi)^{4.24}]$$

and

$$A = [0.4 (R/t) - 3.0]^{0.25} \qquad \text{for } 10 \leq R/t \leq 20$$

and σ_b is the applied FIV axial stress range (psi, peak-to-peak) at a section near the riser flaw. R, t, and α are the pipe mean radius (inch), pipe wall thickness (inch) and flaw half-angle (radians), respectively. The R/t value for the riser pipe is 17.

The FIV fatigue growth threshold crack length ($2R\alpha$) is calculated iteratively such that the calculated value of ΔK is equal to or less than ΔK_{th} value of 5 ksi $\sqrt{in}$. Using the FIV load at

106% RCF and equal loop flows, the calculated fatigue growth threshold crack length is [[ ]], which is [[ ]] longer than the projected circumferential flaw length of [[ ]], as shown in Table 5-4.

5.4.2 FIV Allowable Axial Flaw

Similarly, a through-wall axial flaw is assumed for the FIV fatigue growth "threshold crack length" calculation. The stress intensity factor, ΔK, for a given FIV induced hoop stress range (σ_h, peak-to-peak) is calculated from the relation (References 35 and 38):

$$\Delta K = \sigma_h (\pi a)^{0.5} G_m$$

where

a is half of the axial flaw length (inch),

$$G_m = 0.864 \times a/(Rt)^{0.5} + 0.7 \quad \text{for} \quad a/(Rt)^{0.5} > 0.7$$

and R and t are the pipe mean radius (inch) and pipe wall thickness (inch), respectively.

The FIV fatigue growth threshold crack length (2a) is also calculated iteratively such that the calculated value of ΔK is equal to or less than ΔK_{th} value of 3 ksi $\sqrt{in}$. Using the peak-to-peak pressure differential range of 13.48 psi, scaled from the pressure differential given in Reference 4, the calculated hoop stress range (σ_h, peak-to-peak) is 236 psi. The calculated axial FIV fatigue growth threshold crack length at 106% RCF is [[ ]], which is [[ ]] longer than the projected axial flaw length of [[ ]], as shown in Table 5-4.

5.5 Limit Load Allowable Flaw Length Evaluation

The LL allowable flaw length calculation is a standard calculation methodology provided in BWRVIP-41 Revision 3 (Reference 19) and the ASME Section XI Appendix C (Reference 10). In this analysis BWRVIP-41 was used as the primary source, and if minor differences in the two approaches existed BWRVIP-41 was followed. BWRVIP-41 does not include a LL allowable flaw length evaluation method for axial flaws. Therefore ASME code equations were used with a conservative safety factor of three applied to the loads.

The LL allowable circumferential flaw length calculation was carried out using the load combinations shown in Table 5-3 (References 19 and 39). The loads at the riser pipe section of interest were calculated using a JP finite element model which was subjected to CGS site specific loads.

The hydraulic loads were calculated at 112.2% RCF and crudded JP conditions. The FIV loads were scaled for 112.2% core flow. Allowable flaw lengths were calculated for axial flaws by solving for the crack length which would make the allowable bending stress and the applied

bending stress equal. The allowable axial flaw length was calculated directly using ASME Section XI Appendix C (Reference 10) equations. Note that loads used for the LL analysis were calculated at 112.2% RCF while the loads for the FIV analysis were at 106% RCF.

Table 5-3 Load Combinations Considered for Limit Load Analysis (References 19 and 39)

Service Level (Operating Condition)	Load Combination
A/B (Normal/Upset)	NL + (N-DELTA P) + OBE + SRV + FIV
C (Emergency)	NL + (U-DELTA P) + CHG + SRV
D (Faulted)	NL + (A-DELTA P) + JR + AP + SSE

Definitions:

NL	Metal + Water Weight + Hydraulic Loads (at 112.2% RCF) + Pressure Reaction Loads
OBE	Operational Basis Earthquake
SSE	Safe Shutdown Earthquake
CHG	Chugging Loads
SRV	Safety/Relief Valve Discharge Caused Loads (maximum of symmetric and asymmetric cases)
FIV	FIV Loads (at 103% RCF)
N-DELTA P*	Normal Delta Pressure Force
U-DELTA P*	Upset Delta Pressure Force
A-DELTA P*	Accident Delta Pressure Force
JR	Jet Reaction Loads
AP	Annulus Pressurization Loads
AC	Acoustic Loads

* The limiting delta pressure force was applied to all service level load combinations.

Using the LL approach the circumferential and axial allowable crack lengths were calculated. The limiting circumferential and axial crack lengths at 112.2% RCF with equal loop flows are [[ ]], respectively, as listed in Table 5-4. The LL circumferential allowable length is [[ ]] longer than the projected circumferential flaw length of [[ ]] and axial allowable is [[ ]] longer than the projected axial flaw length of [[ ]], as shown in Table 5-4.

Table 5-4 Summary of Calculated Allowable Flaw Lengths and Comparison with the Projected Flaw Component Lengths

Flaw Length	Circumferential Flaw	Axial Flaw
Existing Flaw Projected after 1 Cycle	[[	
FIV Fatigue Allowable Length (106% RCF)		
Allowable Flaw/Projected Flaw (FIV) (106% RCF)		
LL Allowable Length (112.2% RCF)		
Allowable Flaw/Projected Flaw (LL) (112.2% RCF)		]]

The projected circumferential length of the flaw after one cycle of operation is [[ ]]. The projected axial length of the flaw after one cycle of operation is [[ ]]. Table 5-4 shows that for operation at 106% RCF, the FIV allowable circumferential length is [[ ]] and the FIV allowable axial length is [[ ]]. Both component allowable lengths are greater than the respective projected component length of the flaw after one cycle, as represented by the ratio of the allowable flaw length to the projected flaw length being greater than one. The LL evaluation considered a conservative and bounding RCF of 112.2% RCF. For operation at 112.2% RCF, the LL allowable circumferential length is [[ ]] and the LL allowable axial length is [[ ]]. Both component allowable lengths are greater than the respective projected component length of the flaw after one cycle, as represented by the ratio of the allowable flaw length to the projected flaw length being greater than one.

5.5.1 GEH Safety Communications

SC 09-01 is applicable because the AP loads were calculated based on multiple power-flow points.

In relation to SC 11-07, the new load combination of SSE + (AP + AC) is not in any BWR design/ licensing basis including for CGS. Thus, from the view of the licensing basis, this new load combination can be excluded from this evaluation. The on-going BWR Owners' Group (BWROG) project plans to use the assumption of finite opening break to perform a study to provide a generic disposition for the BWR fleet. Therefore this new load combination is not considered in this evaluation on a plant-specific basis.

In relation to SC 12-20, it should be noted that the AC loads are bounded by the AP loads. GEH Potentially Reportable Concern (PRC) 12-39 identified an error in the method of characteristics

(MOC) approach code used in generating JP AC loads that increased the AC loads by a factor of two. To ensure that the AP loads still bound the AC loads at the location of the flaw, the effective force and moment on the JPs due to AC loads were evaluated further. The correct AC loads were calculated per SC 12-20 and used in this evaluation. The correct AC loads are bounded by the AP loads. Therefore, AC loads are not in the bounding load combination listed in Table 5-3. AC loads have no effect on this flaw evaluation. It was found that the AC loads at the RS-9 weld are less than 10% of the AP loads and thus are bounded by the AP loads (Reference 7).

The AC load values calculated for the evaluation used AC loads not flow induced loads (FIL). Therefore the "not formally" issued GEH SC 14-02 is addressed in this evaluation.

6.0 Leakage Assessment

The leakage flow evaluation performed for References 5 and 6 at the 100% RCF and 112.2% RCF points at the CLTP of 3,486 MWt (Reference 8) bounds the 106% RCF conditions for this evaluation. The results of those evaluations are summarized below.

The two-loop operation case was analyzed for a conservative crack length of [[ ]], which bounds the expected crack length after one cycle of [[ ]]. The crack width was conservatively assumed to be [[ ]]. Because the crack indication is located on the riser pipe there is no effect on the safety function of the JPs to maintain 2/3 core coverage.

The riser crack leakage flow was evaluated using the pressure differential across the riser pipe that was calculated for the CGS hydraulic loads and pressure differential analysis specified in Reference 34. The leakage evaluation was performed using both the BWRVIP-41 Revision 3 (Reference 19) methodology and the GEH proprietary methodology. The results of the leakage evaluation are shown in the following Table 6-1.

Table 6-1 Leakage Evaluation Results

Leakage Evaluation Methodology	100% RCF			112.2% RCF		
	Leakage Flow Rate (gpm)	Core Flow Reduction (%)	JP Flow Reduction (%)	Leakage Flow Rate (gpm)	Core Flow Reduction (%)	JP Flow Reduction (%)
BWRVIP-41, Revision 3 Methodology	112.5	0.131	0.262	125.4	0.131	0.261
GEH Proprietary Methodology	91.3	0.106	0.213	101.8	0.106	0.212

The maximum leakage flow using the BWRVIP-41 (Reference 19) methodology was calculated for maximum possible core flow at 112.2% RCF. For this case, the maximum leakage flow rate through the crack indication was calculated as 125.4 gpm. This leakage flow represents a

0.13% reduction in overall core flow and a 0.26% reduction in the total JP drive flow for the affected recirculation loop. The leakage flow rate for the 100% RCF case was calculated as 112.5 gpm, which represents a 0.13% reduction in overall core flow and a 0.26% reduction in the total JP drive flow for the affected recirculation loop.

The maximum leakage flow using the GEH proprietary methodology was calculated for maximum possible core flow at 112.2% RCF. For this case, the maximum leakage flow rate through the crack indication was calculated as 101.8 gpm. This leakage flow represents a 0.11% reduction in overall core flow and a 0.21% reduction in the total JP drive flow for the affected recirculation loop. The leakage flow rate for the 100% RCF case was calculated as 91.3 gpm, which represents a 0.11% reduction in overall core flow and a 0.21% reduction in the total JP drive flow for the affected recirculation loop.

The more conservative leakage flow rates produced by the BWRVIP-41 (Reference 19) methodology are approximately 23% larger than the flow rates calculated using the GEH proprietary methodology. However both methods demonstrate only a minor effect on JP and core flow.

7.0 Conclusions

To support long-term operation at 106% RCF, an IGSCC crack growth rate of [[ ]], which less than the 5 x 10^{-5} in/hr crack growth rate per Reference 4 is used. The reduced IGSCC crack growth rate justification is based on an evaluation of [[

]] 5 x 10^{-5} in/hr rate.

FIV loads were calculated at the riser pipe near the RS-9 weld by using the plant start-up test data of the original design base configuration. The peak FIV loads were obtained by [[ ]] from significant modes of FIV. These baseline loads were further adjusted to account for the increase of core flow to arrive at an upper bound of FIV loads (Reference 14).

Using the FIV loads at 106% RCF with equal loop flows, the fracture mechanics evaluation was performed to determine the fatigue growth threshold flaw length. The FIV fatigue allowable flaw length was calculated such that the resulting stress intensity factor is equal to the threshold stress intensity factor, ΔK_{th}. For the present evaluation, ΔK_{th} values of 5 ksi $\sqrt{in}$ and 3 ksi $\sqrt{in}$ (Reference 35) were used, respectively, for the circumferential and axial components of the flaw (see Section 5.4 for additional detail).

Using the FIV load at 106% RCF and equal loop flows, the calculated circumferential fatigue growth threshold crack length is [[ ]], which is [[ ]] longer than the projected circumferential flaw length of [[ ]]. The calculated axial FIV fatigue growth threshold crack length at 106% RCF is [[ ]], which is [[ ]] longer than the projected axial flaw length of [[ ]], as shown in Table 5-4. If the crack grows to lengths greater than the maximum allowable flaw lengths provided in this evaluation for 106% RCF, additional evaluations will be necessary.

A LL analysis was also performed to calculate an allowable flaw size to assure no plastic collapse or failure under the normal operating and design accident loads. Using the LL approach the circumferential and axial allowable crack lengths were calculated. The limiting circumferential and axial crack lengths at 112.2% RCF are [[ ]] and [[ ]], respectively, leading to the allowable flaw length to projected flaw length ratios listed in Table 5-4. Comparing the circumferential (1.25 inches) and axial (2.45 inches) crack lengths to the allowable crack lengths it can be concluded that there will not be a catastrophic failure of the riser pipe for any service conditions.

The results of the leakage assessment indicated that JP-17/18 crack leakage has a negligible effect on core flow and a minor effect on JP flow (Reference 7).

For long term operation, GEH recommends that the loop flow in Loop B, where JP-17/18 are located should not exceed one half (½) of the total core flow at 106% of the RCF (½ of 115 Mlbs/hr or 57.5 Mlbs/hr) during balanced flow operation. The loop flow in Loop A may exceed 57.5 Mlbs/hr provided the Technical Specifications on loop flow imbalance are not violated. The loop flows maybe averaged over a one hour time period. It is recommended that whenever possible, the rated power be obtained at a lower core flow, while taking into consideration the core resistance effects. The plant can transition to higher core flows at the end of the fuel cycle when the core resistance is lower, as long as the loop flow in Loop B does not exceed 57.5 Mlbs/hr.

The as-found indication (1.25 inches measured length) is acceptable for one cycle (two years in duration) of operation considering 106% RCF. To account for long-term operation, re-inspection is required at every outage and if the indication's measured length of 1.25 inches does not increase, this evaluation can be used for the next cycle.

8.0 References

1. 1. "Energy Northwest Columbia Generating Station RFO20 Jet Pump 17 Riser Pipe Indication Mechanical Analysis JCO," GE Hitachi Proposal 1-2NBZ10-KK1, Revision 0, May 2011. Legacy DRF Section 0000-0134-3404-R1.

   2. "Energy Northwest Columbia Generating Station Jet Pump 17/18 Evaluation with Full Core Flow," GE Hitachi Proposal 319773, May 2014. PLM DOC-0001-9722-01.

2. 1. Brinkman, T., INR CGS-R20-IVVI-11-07 Jet Pump 17 RS-9, "Columbia Generating Station Spring 2011 Outage CGS R20, "May 2011. Legacy DRF Section 0000-0134-3404-R1.

   2. Goss, E., INR CGS-R21-IVVI-13-01 Revision 2 Jet Pump 17 RS-9, "Columbia Generating Station Spring 2013 Outage CGS R21, "May 2013. PLM DOC-0003-3930.

3. Email from Eddie Wall (GEH) to Andy Meyers (GEH), "RE: CGS JP Riser Flaw Angle," June 24, 2011. Legacy DRF Section 0000-0134-3404-R1.

4. Wirtz, C. and R. Stark, "Superseded 'Needed' Guidance Regarding Crack Growth Assumptions", BWRVIP Letter 2012-074, PLM DOC-0003-3930 Revision 0.

5. GE Hitachi Nuclear Energy, "Justification for Continued Operation (JCO) for Columbia Generating Station with Jet Pump 17/18 Riser Pipe Flaw," NEDC-33689P, October 2011.

6. GE Hitachi Nuclear Energy, "Energy Northwest Columbia Generating Station Long Term Assessment of Columbia Generating Station Jet Pump 17/18 Riser Pipe Flaw at RS-9," 0000-0155-2198-R0, March 2013.

7. GE Hitachi Nuclear Energy, "Columbia Generating Station JP-17/18 Riser Crack Indication Leakage Evaluation Addendum 1," 0000-0134-3400, Revision 3, January 2013.

8. John Bennion (GEH) to Michael Williams (GEH), "Columbia Generating Station Jet Pump 17/18 Riser Pipe Crack Indication Revised Leakage Flow Evaluation using a 3.00-inch Crack Length per CGS JP 17/18 Long-Term Assessment Project Work Plan and Revision to NEDC-33699P," 0000-0134-3400-R3, January 25, 2013.

9. GEH Drawing 795E700 P001, P002, "Jet Pump Modification."

10. ASME Boiler and Pressure Vessel Code, Section XI, Rules for Inservice Inspection of Nuclear Plant Components (Subsection IWB and Appendix C), 2001 Edition / 2003 Addenda.

11. 1. Email from Bilal Khayyat (Energy Northwest) to Andy Meyers (GEH), "RE: CGS JP 17/18 RS-9 JCO – GEH Contacts," July 1, 2011.

2. "Relative Comparison of Indication Length by Using the Same Weld Bead Width in Each Image."

3. "JP-17 auxiliary wedges installed," JP17auxwedge-new.pdf.

12. Goss, E., INR CGS-R20-IVVI-11-03 Jet Pump Wedges and Set Screws, "Columbia Generating Station Spring 2011 Outage CGS R20," May 2011, Legacy DRF Section 0000-0134-3404.

13. 1. "Columbia Jet Pump Inspection and Modification History", Legacy DRF Section 0000-0134-3404-R1.

2. "Attachment 8.1: CGS Jet Pump Riser Brace Cumulative Fatigue Usage Factor Penalties Resulting From Excessive Restrainer Bracket Set Screw Gaps", TM-2144 Revision 2, Page 600, Legacy DRF Section 0000-0134-3404-R1.

14. Chen, CS and A. Huang, "Columbia Jet Pump 17 Weld RS-9 FIV loading for JCO Evaluation," 0000-0134-3395-R3, October 2012.

15. BWRVIP-28-A: "BWR Vessel and Internals Project Assessment of Jet Pump Riser Elbow to Thermal Sleeve Weld Cracking" EPRI, Palo Alto, CA: 2002, 1006601.

16. GE Hitachi Nuclear Energy, "Columbia Generating Station Spring 2011 Outage CGS 20 – JCO Evaluation for Jet Pump 17 Riser Flaw Near the RS-9 Weld," DIR, Revision 4, Legacy DRF Section 0000-0134-2316-R1.

17. "Jet Pump Riser 17/18 Evaluation at Full Rated Core Flow," GE Hitachi Project Work Plan, Revision 0, June 2014. PLM 001N0006.

18. 1. GE Hitachi Nuclear Energy, "CGS JP 17/18 Long Term Assessment and Revision to NEDC 33689P – Revise GEH report NEDC-33689P," DIR, Revision 0, Legacy DRF Section 0000-0134-2316-R2.

2. GE Hitachi Nuclear Energy, "Jet Pump Riser 17/18 Evaluation at Full Rated Core Flow," DIR, PLM 0001N6043 Revision 1.

19. BWRVIP-41, Revision 3: "BWR Vessel and Internals Project, BWR Jet Pump Assembly Inspection and Flaw Evaluation Guidelines," EPRI, Palo Alto, CA: 2010, 1021000.

20. "CGS JP 17/18 Long Term Assessment and Revision to NEDC 33689P," GE Hitachi Project Work Plan, Revision 1, August 2012. Legacy DRF 0000-0151-1673-R1.

21. GE Hitachi Nuclear Energy, "Energy Northwest Columbia Generating Station APRM/RBM/Technical Specifications/Maximum Extended Load Line Limit Analysis (ARTS/MELLLA)," NEDC-33507P, Revision 1, January 2012.

22. GE Company, "Flow-Induced Vibration Characteristics of the BWR/5-201 Jet Pump," NEDE-24153, January 1979.

23. GE Company, "Hanford-2 Reactor Internals Vibration Measurements," NEDE-30995P, May 1985.

24. GEH Drawing 117C2809, "Pipe first made for Jet Pump," December 1967. Legacy DRF Section 0000-0134-3404-R1.

25. GEH Drawing 762E238, "Riser first made for Jet Pump," December 1972. Legacy DRF Section 0000-0134-3404-R1.

26. 1. GE Company, "SAP4G07 User's Manual Static and Dynamic Analysis of Mechanical and Piping Components by Finite Element Method," NEDO-10909, Revision 7, December 1979.

    2. "SAP4G07V," GE Program Library, June 1998. (Level 2)

27. Chen, C.S., "Columbia Jet Pump Dynamic SAP Model," 0000-0134-8858-R0, Legacy DRF 0000-0134-2315, June 2011.

28. NRC RG 1.60 Revision 0 "Damping Values for Seismic Design of Nuclear Power Plants," Table 1 "Damping Value."

29. GE Hitachi Rapid Information Communication Services Information Letter, "Single Loop Operation (SLO) at BWRs," RICSIL 092, Revision 0, December 2010.

30. BWRVIP-03, Revision 11: "BWR Vessel and Internals Project, Reactor Pressure Vessel and Internals Examination Guidelines," EPRI, Palo Alto, CA: 2008, 105696.

31. BWRVIP-224, BWR Vessel and Internals Project, Review of BWR Core Spray Inspection Results," EPRI Technical Report 1019063, December 2009.

32. GE International, Inc. "Characterization and Mitigation of L-Grade Stainless Steel SCC Evaluation in BWRs," NEDC-32985P-C, March 2003.

33. "BWRVIP-174, Revision 1: BWR Vessel and Internals Project, Review of BWR Core Shroud UT Re-Inspection Results for Plants Mitigated with NMCA and HWC," EPRI Technical Report 1019062, August 2009.

34. Letter, Bulent Alpay (GEH) to George Depta (GEH), "Jet Pump Hydraulic Load Analysis," Legacy DRF Section 0000-0134-3397-R0, June 21, 2011.

35. Liaw, P.K., Peck, M.G. and Mehta, H.S., "Fatigue Crack Propagation Behavior of Stainless Steels." Report prepared by Westinghouse STC for GE Nuclear Energy, Contact No. 529-88B860X, April 1990 (GE Proprietary).

36. Barsom, J.M. and Rolfe, S. T. "Fracture and Fatigue Control in Structures: Applications of Fracture Mechanics" Prentice-Hall Inc, 2nd Edition, 1987.

37. Zahoor, A. "Ductile Fracture Handbook" Prepared for Novetech Corporation and EPRI, EPRI Report Number NP-6301-D.

38. Rooke, D. P. and Cartwright D.J. "Compendium of Stress Intensity Factors", London, Her Majesty's Stationery Office, 1976

39. "Columbia Generating Station Final Safety Analysis Report," Table 3.9-2w "Jet Pumps", Amendment 57, December 2003, pg. 3.9-158. Legacy DRF Section 0000-0134-3404-R1.

RESUBMITTAL – DEVIATION FROM BWRVIP FLAW EVALUATION REQUIREMENTS FOR JET PUMP RISER INDICATION
Enclosure 3

NON-PROPRIETARY

Enclosure 3 contains Affidavit from GE-Hitachi Nuclear Energy Americas LLC for GEH PROPRIETARY information included in Enclosure 1